Carbohydrate Polymers 107 (2014) 221–231

Contents lists available at ScienceDirect

Carbohydrate Polymers

journal homepage: www.elsevier.com/locate/carbpol

Catalytic synthesis of sulfated polysaccharides. II: Comparative studies of solution conformation and antioxidant activities

Junlong Wang[a,b,*], Shengfan Niu[a], Baotang Zhao[a,b], Tian Luo[a], Die Liu[a], Ji Zhang[a,b]

[a] College of Life Science, Northwest Normal University, Lanzhou 730070, China
[b] Bioactive Products Engineering Research Center for Gansu Distinctive Plants, Lanzhou 730070, China

ARTICLE INFO

Article history:
Received 4 August 2013
Received in revised form 20 February 2014
Accepted 23 February 2014
Available online 12 March 2014

Keywords:
Catalytic synthesis
Sulfated polysaccharides
Solution conformation
Antioxidant activities
Artemisia sphaerocephala

ABSTRACT

Sulfated derivatives of *Artemisia sphaerocephala* polysaccharide (ASP) with high degree of substitution (DS) were synthesized using 4-dimethylaminopyridine (DMAP)/dimethylcyclohexylcarbodiimide (DCC) as catalyst. Size exclusion chromatography combined with multi-angle laser light scattering (SEC-LLS) results showed a decrease in fractal dimension (d_f) values of sulfated ASP (SASP). Compared to ASP and SASP with low DS (0.51–1.01), $SASP_{cata2}$ exhibited an internal structure between rigid rod and random coil with a DS of 1.24. DS had greater influence on its conformation in aqueous solution. Circular dichroism (CD), methylene blue (MB) and Congo red (CR) spectrophotometric method and atomic force microscopy (AFM) results confirmed that the degradation of ASP and $-SO_3H$ groups improved significantly the stiffness of the chains due to the electrostatic effect. Furthermore, antioxidant experiments revealed that high DS could enhance the scavenging activities of radicals and reducing power of SASP in vitro. The extended chain conformation was beneficial to enhance the biological activity of sulfated polysaccharides.

1. Introduction

It is well known that the activities of polysaccharides are depended upon the chemical structure, such as monosaccharide composition, average molecular weight, degree and pattern of substituting groups and solution conformation (Chen, Xu, Zhang, & Kennedy, 2009; Tao, Zhang, Yan, & Wu, 2007; Wu, Li, Cui, Eskin, & Goff, 2012). Water soluble polysaccharides exhibit different chain conformation in solutions, such as random coil, single helix, double helix, triple helix, aggregate and sphere-like conformation (Zhang, Li, Wang, Zhang, & Peter, 2011). It has been shown by Zhang et al. that the relationship between biological activity and solution conformation are complicated due to the structure varieties (Cui et al., 2008; Wang, Zhang, Zhang, & Ding, 2009; Xu, Zhang, et al., 2009; Xu, Chen, Wang, & Zhang, 2009). The conformation of polysaccharides in solutions can be investigated according to the theory of dilute polymer solutions. Considerable attention has been paid to the solution properties of natural polysaccharides (lentinan and schizophyllan) and the driving force for the conformation transition, such as hydrogen bonding, solvent, temperature and pH value (Tao et al., 2007; Yang and Zhang, 2009; Yi et al., 2012; Zhang et al., 2011). It is reported that triple helix lentinan exhibited a relatively high inhibition ratio against the proliferation of tumor cells, whereas the bioactivity of its single flexible chains almost disappeared (Tao et al., 2007). The results of Chen et al. also indicate that the extended chain conformation were beneficial to enhance the anti-tumor activity, as a result of the increasing of the interaction between polysaccharide and immune system (Chen, Xu, Zhang, & Zeng, 2009). Therefore, a basic understanding of the molecular conformation is essential for successful interpretation of the bioactivities mechanism of water soluble polysaccharides.

Among the natural and synthetic biopolymers, sulfated polysaccharides represent a class of macromolecules of particular interest. The activity of sulfated polysaccharides also depends on structural parameters such as the degree of substitution (DS), the average molecular mass, the position of sulfation and solution conformation (Liu et al., 2009; Wang, Zhang, Zhang, Zhang, & Li, 2009; Wang et al., 2013). It is also shown that the structure of chemical modified polysaccharides is depended on the reaction conditions (Qi et al., 2005). This suggests that upon interaction with reaction reagent, sulfated polysaccharide under-goes complex conformational changes that subsequently modify the biological activities. However, as one of the important factors influencing the activities of sulfated polysaccharide, the studies on the relation between chemical structure and solution conformation have not received much attention in recent articles. Little information on the

* Corresponding author at: College of Life Science, Northwest Normal University, Anning East Road 967, Lanzhou, China. Tel.: +86 0931 7971414; fax: +86 0931 7971414.
E-mail address: nuno-vai@163.com (J. Wang).

http://dx.doi.org/10.1016/j.carbpol.2014.02.074
0144-8617/

conformation of modified polysaccharides with different DS and average molecular mass in aqueous solution has been reported (Wang, Zhang, Zhang, et al., 2009). The main reason is that the building blocks of sulfated polysaccharides are rather complex toward the harsh conditions of sulfation and that some glycosidic linkages can be hydrolyzed relatively easily. Therefore, it is very important to clarify the structures and solution properties of sulfated polysaccharide.

It is the purpose of the present investigation to explore systematically the solution conformation of sulfated polysaccharide with different structure features. In our previous studies, sulfated derivatives of *Artemisia sphaerocephala* polysaccharide (SASP) with high DS were prepared using 4-dimethylaminopyridine (DMAP)/dimethylcyclohexylcarbodiimide (DCC) as catalyst (data is being considered for publication). The chemical structure of SASP was analyzed by FT-IR, X-ray photoelectron spectroscopy (XPS) and ^{13}C NMR spectroscopy. The DS (0.51–1.28) and weight average molecular mass (0.626–4.771 $\times 10^4$ Da) of SASP were listed in Table 1. *A. sphaerocephala* polysaccharide (ASP) and SASP had the same monosaccharide composition (Ara:Xyl:Man:Glc:Gal) but different molar ratio (1:4.21:45.9:9.74:11.43 and 1:5.43:12.41:14.62:6.85, respectively).

The present study is focused on the mechanisms governing the relations between chain conformation and structure features. For that purpose, size-exclusion chromatograph combined with multi-angle laser photometer (SEC-LLS), circular dichroism (CD), methylene blue (MB) and Congo red (CR) spectrophotometric method and atomic force microscopy (AFM) are employed to determine the chain conformation in solution and molecular morphology. Moreover, we also evaluate the effect of DS on the antioxidant activities of SASP in vitro and offer theoretical evidence for the synthesis of sulfate polysaccharides with different structure features. Antioxidant properties are assayed in terms of antioxidant activities in vitro, by testing the scavenging abilities on superoxide radicals, hydroxyl radicals, 1,1-diphenyl-2-picryl-hydrazyl (DPPH) and reducing power.

2. Materials and methods

2.1. Preparation of SASP

ASP was extracted and purified according to our previous studies (Wang, Zhang, & Wang, et al., 2009; Wang et al., 2010). ASP (500 mg) was suspended in anhydrous formamide (30 mL) at room temperature with stirring for 30 min, and the sulfating reagents (chlorosulfonic acid/pyridine) were added dropwise. Then, DMAP and DCC were added. For comparison, sulfation reactions without DMAP and DCC were also studied. The mixture was stirred for 3 h at different temperatures (Table 1). After the reaction, the mixture was cooled to room temperature and the pH value was adjusted to 7–8 with 2 mol/L NaOH solution. The mixtures were precipitated with ethanol (95%), washed, redissolved in water, and then dialyzed (molecular weight cutoff 8–12 kDa) against tap water for 48 h and distilled water for 24 h to remove pyridine, salt and potential degradation products. Sulfated ASP ($SASP_1$–$SASP_5$ for samples without catalyst and $SASP_{cata1}$–$SASP_{cata7}$ for samples using catalyst) with different DS (Table 1) were collected. The samples were stored in a dry box under room temperature till use.

2.2. Molecular mass and size characterization

The most commonly employed method for conformation studies are dynamic and static light scattering technique (Sumihito, Tomoko, & Takashi, 2001; Tomoko & Takashi, 2003; Yi et al., 2012).

Table 1
Molecular properties of ASP and its sulfated derivatives.

Samples	CSA:Pyr	DMAP/DCC (mg)	Temperature (°C)	DS	$M_W \times 10^4$	Relation equation	d_f	Conformation
ASP	–	–	–	–[a]	7.348	$\langle S^2\rangle_z^{1/2} = 0.203M_w^{0.35\pm0.027}$	2.86	Between hard sphere and random coil (fully swollen)
$SASP_1$	1:4	–	40	0.51	3.836	$\langle S^2\rangle_z^{1/2} = 0.309M_w^{0.36\pm0.034}$	2.77	Between hard sphere and random coil (fully swollen)
$SASP_2$	1:2	–	40	0.69	3.203	$\langle S^2\rangle_z^{1/2} = 0.309M_w^{0.36\pm0.034}$	2.63	Between hard sphere and random coil (fully swollen)
$SASP_3$	1:1	–	40	0.82	2.110	$\langle S^2\rangle_z^{1/2} = 0.309M_w^{0.36\pm0.034}$	2.08	Between hard sphere and random coil (not swollen)
$SASP_4$	2:1	–	40	0.87	0.645	$\langle S^2\rangle_z^{1/2} = 0.309M_w^{0.36\pm0.034}$	2.38	Between hard sphere and random coil (not swollen)
$SASP_5$	2:1	–/200	40	0.91	1.353	$\langle S^2\rangle_z^{1/2} = 0.309M_w^{0.36\pm0.034}$	1.96	Random coil
$SASP_{cata1}$	2:1	5/200	40	0.83	2.382	$\langle S^2\rangle_z^{1/2} = 0.29M_w^{0.37\pm0.048}$	2.70	Between hard sphere and random coil (fully swollen)
$SASP_{cata2}$	2:1	10/200	40	1.24	3.103	$\langle S^2\rangle_z^{1/2} = -1.99M_w^{0.88\pm0.55}$	1.13	Between rigid rod and random coil
$SASP_{cata3}$	2:1	20/200	40	1.01	1.292	$\langle S^2\rangle_z^{1/2} = -0.056M_w^{0.43\pm0.017}$	2.32	Between hard sphere and random coil (not swollen)
$SASP_{cata4}$	2:1	50/200	40	0.98	2.002	$\langle S^2\rangle_z^{1/2} = -0.023M_w^{0.31\pm0.005}$	3.22	Hard sphere
$SASP_{cata5}$	2:1	100/200	40	0.82	4.771	$\langle S^2\rangle_z^{1/2} = 0.218M_w^{0.37\pm0.029}$	2.70	Between hard sphere and random coil (fully swollen)
$SASP_{cata6}$	2:1	10/200	60	1.28	3.097	$\langle S^2\rangle_z^{1/2} = 0.26M_w^{0.28\pm0.036}$	3.57	Hard sphere
$SASP_{cata7}$	2:1	10/200	90	1.13	0.626	$\langle S^2\rangle_z^{1/2} = 0.723M_w^{0.15\pm0.018}$	6.67	Hard sphere

[a] Not detected.

Therefore, we investigated the molecular mass and solution conformation of ASP and its derivatives more in depth by the combination of SEC and the quantitative detection using multi-angle laser photometer.

SEC-LLS measurements were carried out on size-exclusion chromatograph combined with multi-angle laser photometer (MALLS, λ = 690 nm; DAWN EOS, Wyatt Technology Co., USA). Ultrahydrogel™ column (7.8 × 300 mm, Waters, USA) was used. An optilab refractometer (Dawn, Wyatt Technology Co., USA) was simultaneously connected. ASP and its derivatives with desired concentrations (0.01 mg/mL) were prepared (dissolved in ultrapure water) and optical clarification of these samples was achieved by filtration into a scattering cell. The injection volume was 50 μL and the flow rate was 0.5 mL/min (mobile phase of ultrapure water). The refractive index increment (d_n/d_c) value of the sample was determined by using an optilab refractometer at 690 nm (25 °C) to be 0.145 mL/g. The basic light scattering equation was as follows

$$\frac{KC}{R_\theta} = \frac{1}{M_w}\left(1 + \frac{16\pi^2\langle S^2\rangle_z}{3\lambda^2}\cdot\sin^2\left(\frac{\theta}{2}\right)\right) + 2A_2C \quad (1)$$

where K was an optical constant equal to $[4\pi^2 n_0^2 (d_n/d_c)^2]/(\lambda^4 N_A)$; C, the polysaccharide concentration in mg/mL; R_θ, the Rayleigh ratio of the scattered to incident light intensity; M_W, the average molecule weight; λ, the wavelength of incident light; n_0, the refractive index of the solvent; d_n/d_c, the refractive index increment; N_A, the Avogadro' number; A_2, the second virial coefficient; $\langle S^2\rangle_z$, the mean square radius of gyration; θ, the scattering angle. As the column separated the polymer according to molecular size, each fraction was led to the light scattering detector for instantaneous measurement of the scattering intensities. The polymer concentration was calculated based on the peak area determined by the refractive index detector, according to glucan standards.

2.3. Circular dichroism

CD may provide a convenient method of investigating the conformational change of substituted polysaccharides by chromophores (Yang and Zhang, 2009). CD measurements were performed on a Jasco J-810 spectropolarimeter (Jasco Corporation, Tokyo, Japan). A flat faced quartz sample cell of 10 mm optical path length was used and the following set up was maintained: bandwidth, 2 nm; time constant, 2 s; scan rate, 20 nm/min. Three spectra were averaged for each sample. All experiments were performed at 25 °C. The polysaccharide aqueous solutions (1.0 mg/mL) were scanned three times accumulation time, and all observations were repeated at least three times.

2.4. Methylene blue and Congo red spectrophotometric method

Methylene blue (MB) and Congo red (CR) spectrophotometric method has been commonly used to determine the shift of maximum absorption wavelength when combine with helical polysaccharides, as a technique to identify molecular conformation of water soluble polysaccharides (Antonov & Sato, 2009; Michon, Konate, Cuvelier, & Launay, 2002; Rout, Mondal, Chakraborty, & Islam, 2008).

The procedure of methylene blue spectrophotometric (MBS) method was adapted from Antonov and Michon et al. A methylene blue (MB) solution in phosphate buffer (pH 7.3) was prepared by stirring at room temperature for 1 h. The solution concentration was adjusted (0.0005 wt%) so that its absorption at 664 nm (A_{664nm} at 20 °C) had a value of about 0.7–0.8. MB/SASP solutions were prepared by adding the different amount of the stock solution of SASP in the MB solution and by stirring at 70 °C for 10 min and then at 80 °C for 20 min. Series of MB/SASP solutions were prepared in the range of SASP concentrations from 0.01 to 1 mg/mL (A_{663nm} value remained lower than 1.0). Optical density sweeps as a function of the wavelength in the range 450–750 nm were performed at selected temperature in 1 cm glass cells using a UV/vis spectrophotometer (UV1000, Labtech).

The procedure of Congo red spectrophotometric (CRS) method was adapted from Rout et al. SASP solution (2 mL, 0.2∼2 mg/mL) was mixed with 2 mL CR (91 μmol/L) and 1 mL NaOH solution (final concentration of NaOH, 0.2–2 mol/L). Meanwhile, 2 mL CR (91 μmol/L) was mixed with 1 mL NaOH solution as the control. Maximum absorption wavelength (λ_{max}) was measured in the range from 400 to 600 nm after equilibrating for 10 min at room temperature (UV1000, Labtech).

2.5. AFM

AFM particularly permits nondestructive imaging of soft biological surface. It has been widely adopted to explore the molecular and supramolecular structures of biological macromolecules (Yi et al., 2012). ASP and SASP were dissolved in HPLC grade water and serially diluted to the desired concentration (1 μg/mL and 20 μg/mL). Two microlitres of the solution were pipetted onto a freshly cleaved 10 mm diameter disk of mica and air dried. The mica was mounted in a Multimode Scanning Probe microscope with a Nanoscope IIId controller, operated as an atomic force microscope in the Tapping Mode (Veeco Instruments, USA).

2.6. Assay for antioxidant activities

2.6.1. Effect of scavenging 1,1-diphenyl-2-picryl-hydrazyl (DPPH) radicals

The free radical scavenging activity of the polysaccharides was measured by DPPH test according to the method of Shimada et al. with some modifications (Shimada, Fujikawa, Yahara, & Nakamura, 1992). The solution of DPPH in methanol (0.2 mmol/L) was prepared daily before UV measurements. Polysaccharides were dissolved in deionized water at the concentration of 0.02–5 mg/mL. The sample solutions were thoroughly mixed with 2 mL of freshly prepared DPPH and 2 mL of methanol. The mixture was shaken well, allowed to stand for 30 min in the dark, and the absorbance was then measured at 517 nm against a blank. Lower absorbance of the reaction mixture indicated higher free radical scavenging activity, which was analyzed from the graph plotted of inhibition percentage against compound concentration. V_c was used as positive controls. The experiments were carried out in triplicate and averaged. The capability to scavenge the DPPH radical was calculated using the following equation:

$$\text{Scavenging effect}\ (\%) = \left[A_0 - \frac{A - A_b}{A_0}\right] \times 100\%$$

where A_0 was the absorbance of DPPH solution without sample; A was the absorbance of the test sample mixed with DPPH solution and A_b was the absorbance of the sample without DPPH solution.

2.6.2. Superoxide radical scavenging assay

The superoxide radical scavenging assay was measured according to the reported method (Qi et al., 2005). Superoxide radicals were generated in a phenazine methosulfate (PMS)/nicotinamide adenosine denucleotide hydro-phosphoric acid (NADH) system. Polysaccharides were dissolved in deionized water at the concentration of 0.02–5 mg/mL. The reaction mixture, containing varying concentrations of samples, Tris–HCl (16 mM, pH 8.0), NADH (338 μM), *p*-nitro blue tetrazolium chloride (NBT, 72 μM) and PMS (30 μM) was incubated at room temperature for 5 min and the absorbance was recorded at 560 nm against a blank. The capability

to scavenge superoxide radical was calculated using the following equation:

$$\text{Scavenging effect}\ (\%) = \left[1 - \frac{A}{A_0}\right] \times 100\%$$

where A_0 was the absorbance of mixture solution without sample; A was the absorbance of the test sample mixed with reaction solution.

2.6.3. Hydroxyl radical scavenging assay

The hydroxyl radical assay was measured by the reported method (Ghiselli, Nardini, Baldi, & Scaccini, 1998) with a minor modification. Polysaccharides were dissolved in deionized water at the concentration of 0.1–5 mg/mL. The sample solution (0.1 mL) was mixed with 0.6 mL of reaction buffer [20 mM phosphate buffer (pH 7.4), 2.67 mM deoxyribose, and 100 μM EDTA], 0.2 mL of 0.4 mM ferrous ammonium sulfate, 0.05 mL of 2.0 mM V_c, and 0.05 mL of 10 mM H_2O_2 was then added to the reaction solution. The reaction solution was incubated for 15 min at 37 °C and then 1 mL of 1% thiobarbituric acid (TBA) and 1 mL of 2% trichloroacetic acid (TCA) were added to terminate the reaction. The mixture was boiled for 15 min and cooled to room temperature. The absorbance of the mixture was measured at 532 nm against blank. The capability to scavenge hydroxyl radical was calculated using the following equation:

$$\text{Scavenging effect}\ (\%) = \left[1 - \frac{A}{A_0}\right] \times 100\%$$

where A_0 was the absorbance of mixture solution without sample; A was the absorbance of the test sample mixed with reaction solution.

2.6.4. Reducing power assay

The reducing power was determined according to the method of Qi et al. (2005). Different concentrations of samples (0.1–5 mg/mL, 2.5 mL) was mixed with 2.5 mL of 0.2 M sodium phosphate buffer (pH 6.6) and 2.5 mL of potassium ferricyanide (1%). The mixture was incubated for 20 min at 50 °C. The reaction was terminated by TCA solution (10%). Then, the solution was mixed with distilled water and ferric chloride (0.1%), the absorbance was measured at 700 nm against a blank. A higher absorbance indicated a higher reducing power. BHA was used for comparison.

2.6.5. Statistical analysis

All the data were repeated 3 times and presented as mean ± S.D. P value of less than 0.05 was considered significant. Statistical evaluations and EC_{50} values in all experiments were performed by SPSS software 17.0.

3. Results and discussion

3.1. Analysis of molecular properties

In the present study, we used sulfated samples with different molecular weight and DS to study how molecular weight and DS affected conformation in aqueous solution. Our results showed that sulfated derivates with different DS and molecular weight were obtained by changing the reaction conditions. Compared to the native one, all the samples showed a sharp decrease in M_w due to the extensive degradation of the polysaccharides during the sulfation (Table 1). Relevant structural information and further insight into the nature of the polysaccharide could be obtained by investigating the fractal dimension (d_f) (Tao, Zhang, & Peter, 2006). The d_f value could be determined from the M_w dependence of $\langle S^2\rangle_z^{1/2}$, and was defined as the inverse of the exponent ν:

$$\langle S^2\rangle_z^{1/2} = fM^{\nu} \quad (2)$$

$$d_f = \frac{1}{\nu} \quad (3)$$

On the basis of the theory of polymer solutions, the value of d_f was 1 for a rigid rod, and linear polymers with Gaussian coil nature had d_f value ranging from 5/3 to 2. A three-dimensional object with a homogeneous density had a mass fractal dimension of 3. The d_f value of monodisperse polymers could be extracted directly from the angular dependence of the scattered light or neutron intensity. This approach had been successfully applied to highly branched polysaccharides with high molecular size such as amylopectin and other synthetic branched polymers (Tao & Xu, 2008; Wang et al., 2011).

The straight line fitting of the experimental data points was shown in Table 1. The ν value of 0.35 suggested that ASP molecules in aqueous solution were in the state between hard sphere and random coil. Furthermore, the value of d_f was calculated to be 2.86 according to Eq. (3). The d_f value of 2.86 was characteristic of a particle having an internal structure between the hard sphere ($d_f = 3.0$) and the fully swollen branched macromolecule in a thermodynamically good solvent ($d_f = 2.0$). The result confirmed that ASP existed as a sphere conformation of branched clusters in aqueous solution.

In sulfated samples, a decrease in d_f values was observed. The d_f values of $SASP_3$, $SASP_4$ and $SASP_{cata3}$ were 2.08, 2.38 and 2.32, respectively. A d_f value of 2.08–2.38 was characteristic of a particle having an internal structure between hard sphere and the branched macromolecules which were not swollen, either for thermodynamic reasons or because of steric hindrances (Bauer & Burchard, 1993). In addition, an increase in the ν values of high DS samples was observed (Fig. 1A). The d_f value of 1.96 indicated that $SASP_5$ with high DS exhibited as a random coil conformation in aqueous solution. The ν value of 0.88 for $SASP_{cata2}$ was larger than all of the samples. The d_f value of 1.13 indicated that $SASP_{cata2}$ exhibited an internal structure between rigid rod and random coil. This value was lower than that of $SASP_2$ with similar molecular weight but lower DS. The result indicated that under the same conditions, SASP with higher DS had a lower ν value. It suggested that DS had greater influence on its conformation in aqueous solution. Our results indicated that sulfated polysaccharides showed less flexibility compared with the native one. It was confirmed by the results of Tao et al. Similar d_f value (1.79) in sulfated polysaccharide showed that the $-SO_3H$ groups in the derivatives enhance the steric hindrance between the polymer chains (Tao et al., 2006). The major driving force for the conformation in aqueous solution was due to the intramolecular hydrogen bonding (Zhang et al., 2011). Low molecular weight and electrostatic effect of $-SO_3H$ groups leading to the relatively expanded conformation of the sulfated derivatives with totally different intramolecular hydrogen bonding compared to the native one (Fig. 1B). Similar result was reported that the introduction of $-SO_3H$ groups strengthens the effect of electrostatic repulsion, resulting in chain expansion and increased stiffness (Zhang, Zhang, Wang, & Cheung, 2003). Chen et al. also found that the introduction of the phosphate groups into the β-glucan improved significantly the stiffness of the chains (Chen, Xu, Zhang, & Zeng, 2009).

Based on the results, it could be concluded that sulfation and degradation occurred simultaneously in the sulfation process (Parvathy, Susheelamma, Tharanathan, & Gaonkar, 2005). Such a feature could be assigned to the fact that intra-molecular repulsive interactions were unneglectable in sulfate polysaccharides (Zou et al., 2008). Higher DS and lower molecular weight might lead to an expanded conformation. It suggested that DS had greater influence on its conformation in aqueous solution. In order to prove unambiguously that DS was an important parameter influencing bioactivity, it was worthwhile evaluating the effect of DS on antioxidant activities. In that regard, antioxidant experiments of SASP

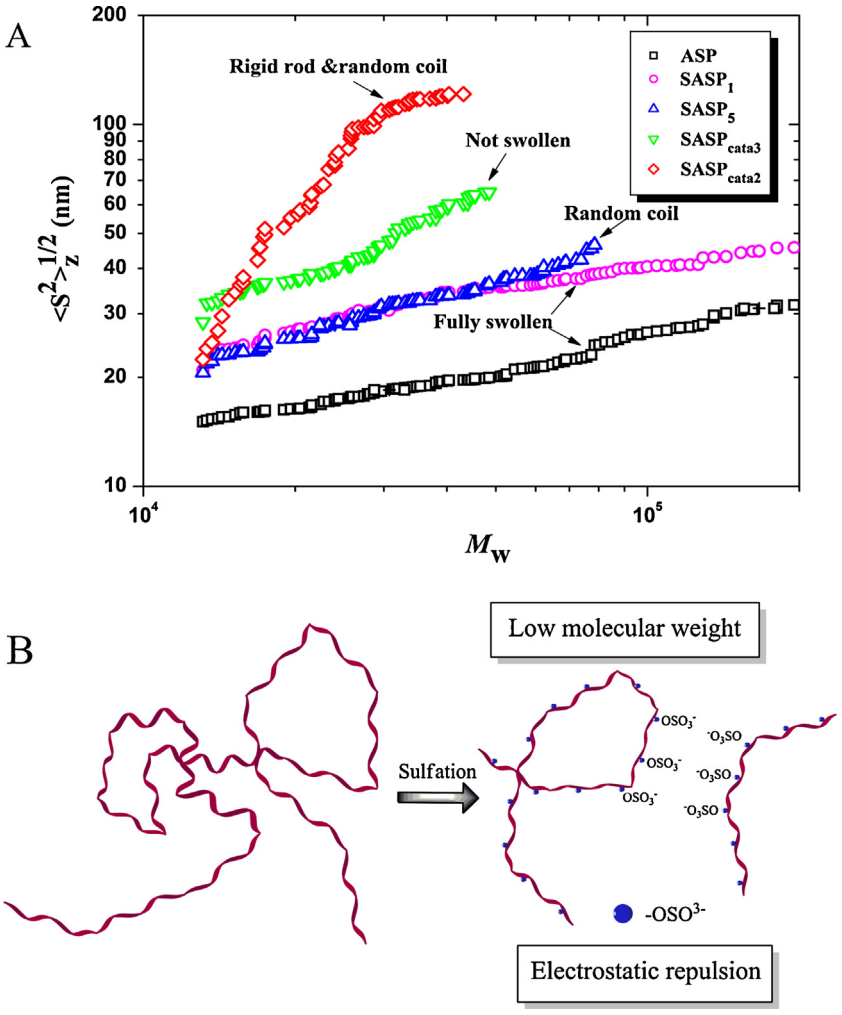

Fig. 1. Plot of log M_w versus $\langle S^2 \rangle_z^{1/2}$ for ASP and its sulfated derivates at 25 °C (A) and schematic representation of conformation transition after sulfated modification (B).

with different DS were employed. The effect of DS on antioxidant activities was shown in Section 3.6.

3.2. Circular dichroism (CD) studies

To determine the conformational changes of the secondary and the local tertiary structures of SASP, CD spectroscopy was applied at neutral pH values. Fig. 2 was the CD spectra of pure ASP solution. ASP solution exhibited a negative band at 209 nm in circular dichroism, which may assign to the carboxylate n–π* transition (Huang, Tan, Zhou, Wang, & Che, 2008). Fig. 2 also showed CD spectra of $SASP_{cata2}$ were dependent on the solution concentration. A red shift of n–π* transition of $SASP_{cata2}$ with decreasing ellipticity at 216 nm was observed. It was proposed that such a decrease in the ellipticity and a red shift of the n-π* transition reflected the appearance of S=O. Therefore, both chain conformation and CD data strongly suggested that the screening of the negative charges on the polysaccharide chain promoted a transition toward a more rigid conformation.

3.3. Methylene blue (MB)/SASP interactions

MB was a good way to indirectly determine the effect of DS on conformational changes of sulfated polysaccharides. Absorption spectra of the MB in aqueous solutions with different SASP concentrations were shown in Fig. 3A and C. In solution without SASP, the spectrum had one peak of absorption at 664 nm and a shoulder at 619 nm. With increasing the $SASP_4$ and $SASP_{cata2}$ concentrations, the peak height at 664 nm decreased and a new peak appeared at 554 nm. The spectrum change indicated the formation of a MB/SASP metachromatic complex might be due to the electrostatic interaction between the positively charged MB and

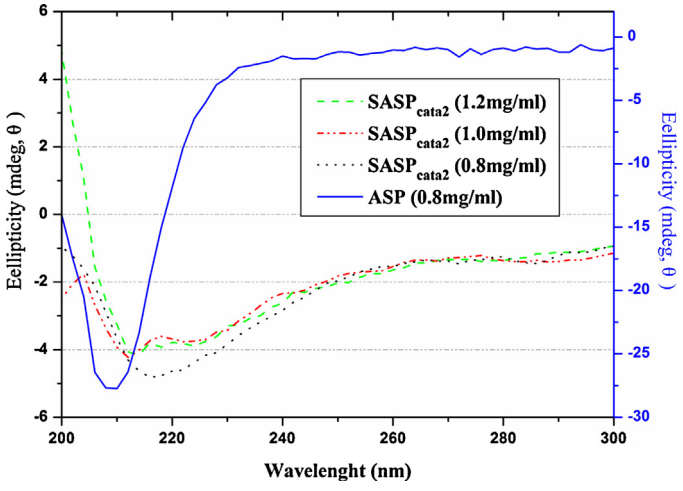

Fig. 2. Circular dichroism spectra of ASP and $SASP_{cata2}$ of different concentration.

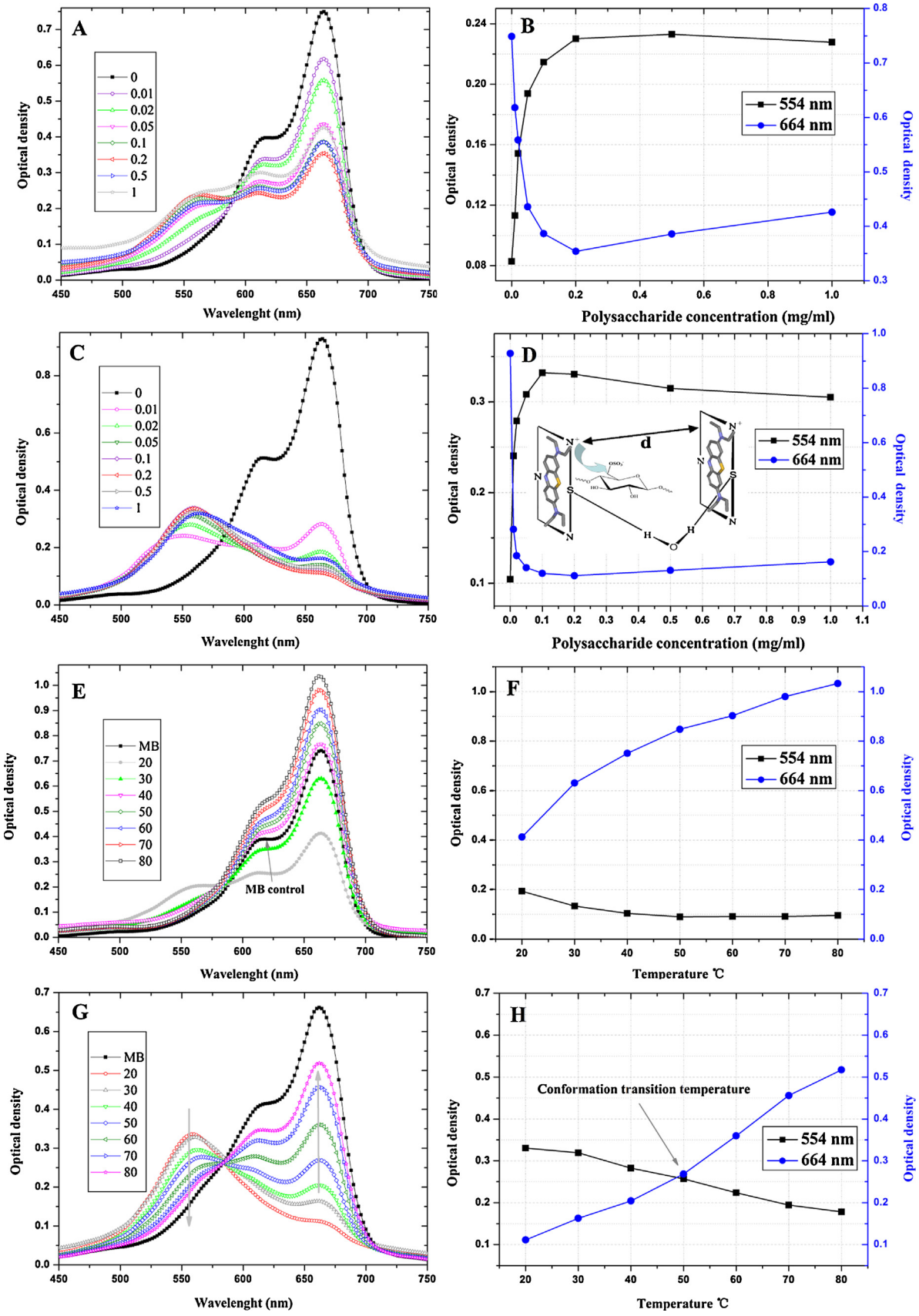

Fig. 3. Evolution of optical density at 664 nm and 554 nm as a function of polysaccharide concentration at 20 °C and temperature at the polysaccharide concentration of 0.2 mg/mL. (A) UV–vis spectrum of $SASP_4$ at 20 °C, (B) optical density of $SASP_4$ at 20 °C, (C) UV–vis spectrum of $SASP_{cata2}$ at 20 °C, (D) optical density of $SASP_{cata2}$ at 20 °C, (E) UV–vis spectrum of $SASP_4$ at the concentration of 0.2 mg/mL, (F) optical density of $SASP_4$ at the concentration of 0.2 mg/mL, (G) UV–vis spectrum of $SASP_{cata2}$ at the concentration of 0.2 mg/mL and (H) optical density of $SASP_{cata2}$ at the concentration of 0.2 mg/mL.

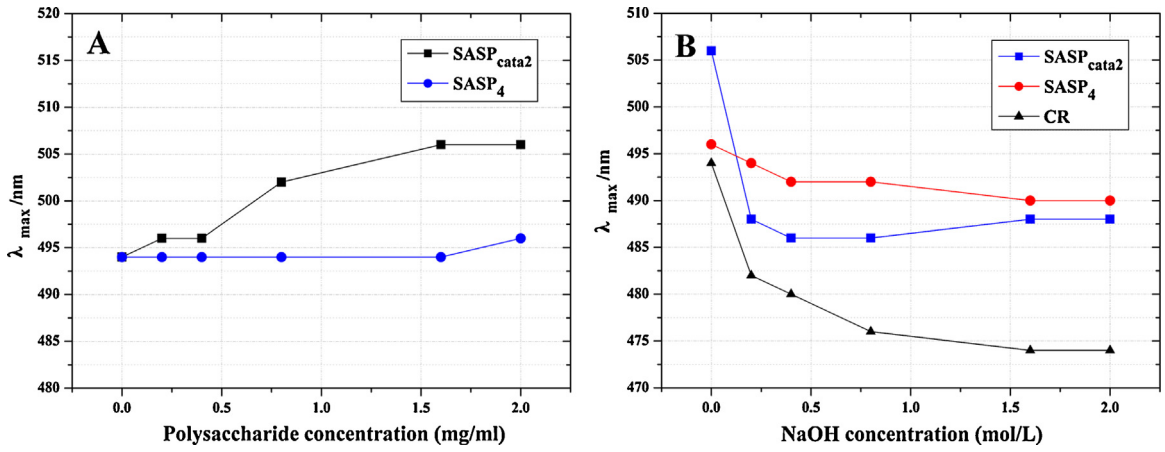

Fig. 4. Optical density of SASP/CR (A) in various polysaccharides concentrations and (B) in various NaOH concentrations at 20 °C.

negatively charged sulfated group on SASP. Since both peaks no longer changed for concentrations higher than 0.2 mg/mL, all the available MB molecules might have completely interacted with sulfate groups at concentrations higher than 0.2 mg/mL (Fig. 3B and D).

Fig. 3E–H showed the evolutions of OD_{664nm} and OD_{554nm} (optical density measured at 664 and 554 nm) as a function of temperature. The levels of OD_{664nm} and OD_{554nm} plateaus were depended on temperature and the larger evolution occurred above 50 °C in $SASP_{cata2}$. With the increase of temperature (20–80 °C), a sharp decrease of OD_{554nm} was observed. These phenomena could be attributed to an increase of polysaccharide chains rigidity. The life time of the long-range forces interactions with H_2O was longer and a larger number of MB molecules were aligned and absorbed at 664 nm instead of 554 nm. This result was in good agreement with those of Michon et al. obtained with MB and carrageenan interactions (Michon et al., 2002). However, no temperature dependence was observed in $SASP_4$, it might be due to the lower DS and more flexible conformation in solution, which was in accordance with SEC-LLS results presented in Section 3.1. The similar conformation transition induced by thermal treatment had been reported by Zhang et al. (2011), showing an irreversible conformational transition from triple helix to single coil appeared at high temperature. Moreover, it could be inferred that the conformational transition temperature was 50 °C in MBS test.

3.4. Congo red/SASP interactions

The complex formation of SASP with CR was evaluated from the shift in the visible maximum absorption of CR at various alkali concentrations. CR in NaOH served as the negative control. Changes in λ_{max} of complex at various concentrations of NaOH were shown in Fig. 4. The red shifts of λ_{max} of the samples were not observed at all concentrations and the curve was flattened even in high concentrations of alkali. However, the initial λ_{max} of $SASP_{cata2}$/CR was obviously higher than that of $SASP_4$/CR and CR. As noted above, $SASP_{cata2}$ with higher M_W (3.103×10^4) and DS exhibited a more rigid conformation. The depolymerization of $SASP_{cata2}$ from single-helix to random coil was happened. Similar result was reported that the depolymerization of rigid conformation to flexible conformation was observed in longan pulp polysaccharide (Yi et al., 2012). Thus, it could be concluded that $SASP_{cata2}$ showed rigid conformation as discussed in SEC-LLS analysis, but not triple-helical conformation in solution. Moreover, the initial λ_{max} of $SASP_4$/CR and negative control was close. Compared to $SASP_{cata2}$, $SASP_4$ showed lower M_W (0.645×10^4) and more flexibility. No characteristic variance of conformation transition was detected. SASP/CR result further revealed that chain rigidity of SASP increased with higher DS.

3.5. AFM

Fig. 5 showed a topographical AFM image of $SASP_{cata3}$ deposited from 1 μg/mL aqueous solution. To avoid tip broadening, we adopted molecular height to characterize the size of polysaccharide in section analysis (Marshall, Hoa, Peter, Madhav, & Arland, 2009). The molecules appeared spherical lumps and somewhat asymmetric in shape. Section analysis showed the height ranged from 0.41 to 4.38 nm with the average height of 0.89 nm. The height of a single polysaccharide chain was about 0.1–1 nm (Tao, Biao, Yu, & Ning, 2008). Particle analysis also confirmed that the most molecules were at one molecule height. Moreover, inter- and/or intra-molecular aggregation was also observed. When deposition was made at a higher polymer concentration (20 μg/mL), irregularly shaped large structures formed compact molecules with heights ranging from 0.97 to 5.54 nm at a mean of around 1.66 nm (Fig. 6). However, neither linear molecule nor network structure was observed in SASP compared to ASP (Zhang et al., 2007). It indicated that a molecular morphology transition during sulfation was happened. This conclusion supported the result of SEC-LLS.

3.6. Antioxidant activity analysis

3.6.1. Scavenging activity of DPPH radicals

The scavenging ability of the samples on DPPH radical was shown in Fig. 7A and compared with V_c. Compared to ASP (EC_{50} of 4.946 mg/mL), all sulfated polysaccharides showed better scavenging effects. $SASP_{cata2}$ had strong antioxidant activity with EC_{50} value of 2.007 mg/mL. The scavenging effects of $SASP_5$ and $SASP_1$ were weaker than V_c (EC_{50} of 0.613 mg/mL) and $SASP_{cata2}$, the EC_{50} values were 4.896 mg/mL and 4.702 mg/mL, respectively. It suggested that the DS of SASP had great influence on its scavenging effects of DPPH radical. It was reported that the effect of antioxidant activities was due to their hydrogen donating ability (Wang, Zhang, Zhang, et al., 2009). The presence of $-OSO_3H$ groups in the SASP molecule could activate the hydrogen atom of the anomeric carbon. The higher activated capacity of the group, the stronger hydrogen atom-donating capacity. It was concluded that $SASP_{cata2}$ with highest DS showed the best scavenging activity of DPPH radicals.

3.6.2. Scavenging activity of superoxide radical

Fig. 7B showed that the inhibitory effect of SASP on superoxide radical was significant at all tested concentrations in a

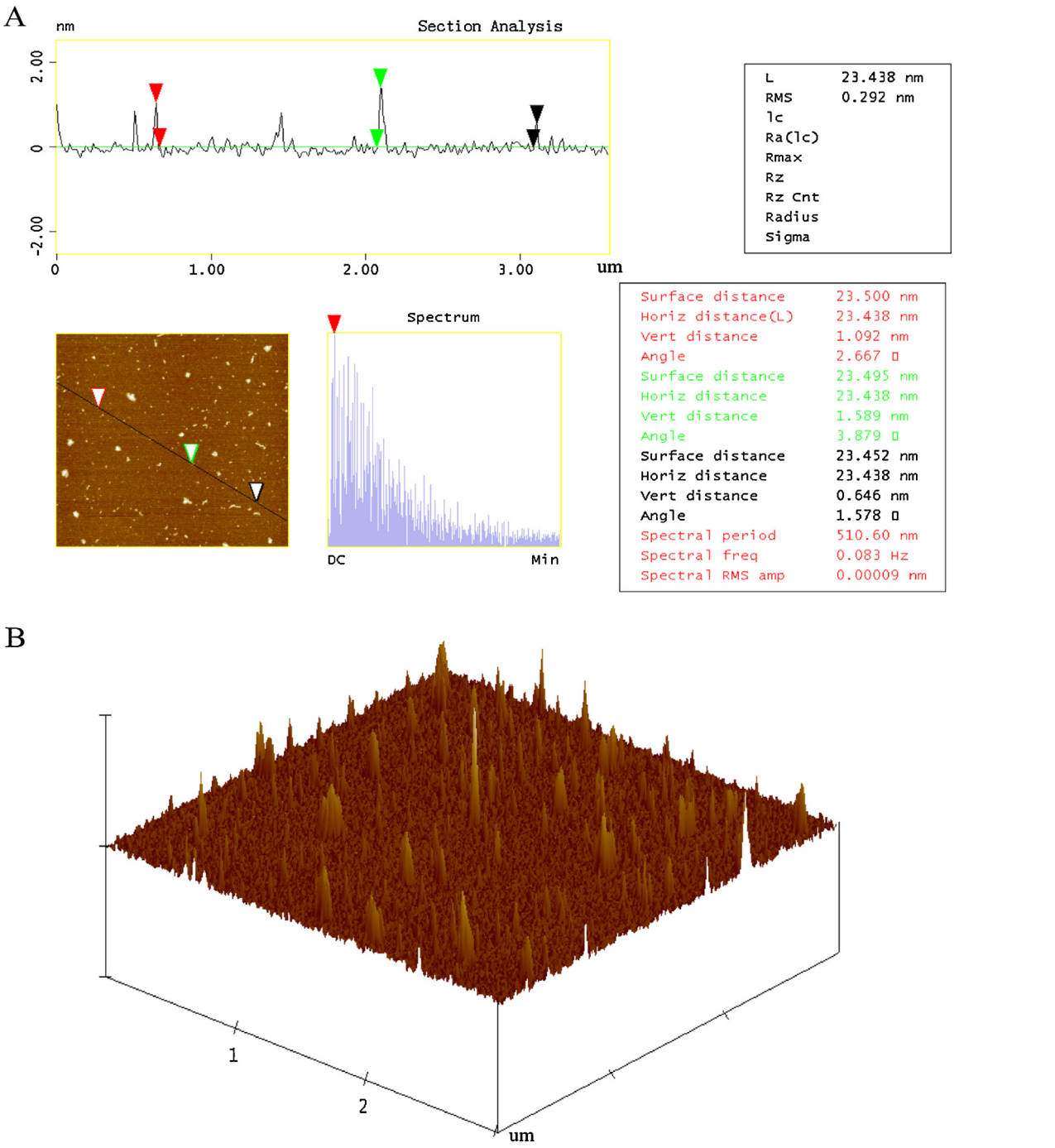

Fig. 5. AFM images of $SASP_{cata3}$ deposited from water at the concentration of 1 μg/mL. (A) 2D map and section analysis. Scale bar was 3 μm; inset height scale was 0–5 nm. (B) 3D map.

concentration dependent manner. The EC_{50} values of $SASP_{cata2}$, $SASP_5$ and $SASP_1$ were 0.027, 0.03 and 0.028 mg/mL, which were higher than V_c (0.077 mg/mL) and ASP (1.013 mg/mL). According to the results, all sulfated samples showed stronger scavenging effect than the native one. This demonstrated that DS affected the antioxidant activity, which was in accordance with Wang et al. that higher sulfate content showed greater scavenging effect of superoxide radical (Wang, Zhang, Zhang, & Li, 2008). Our data on the activity of scavenging superoxide radicals suggested that it was likely to contribute toward the observed antioxidant effect.

3.6.3. Scavenging activity of hydroxyl radical

As shown in Fig. 7C, all the sulfated samples were found to have greater ability to scavenge hydroxyl radicals compared to ASP with EC_{50} value of 6.073 mg/mL. $SASP_{cata2}$ showed the best scavenging ability with the EC_{50} value of 2.14 mg/mL. $SASP_5$ and $SASP_1$ showed lower scavenging effect, and the EC_{50} values were 4.71 and 5.75 mg/mL, respectively. Sulfated derivatives were found to have the scavenging ability in a DS-dependent fashion. Relationship between EC_{50} value and DS was obvious. The result indicated that the sulfate group played an important role in the scavenging

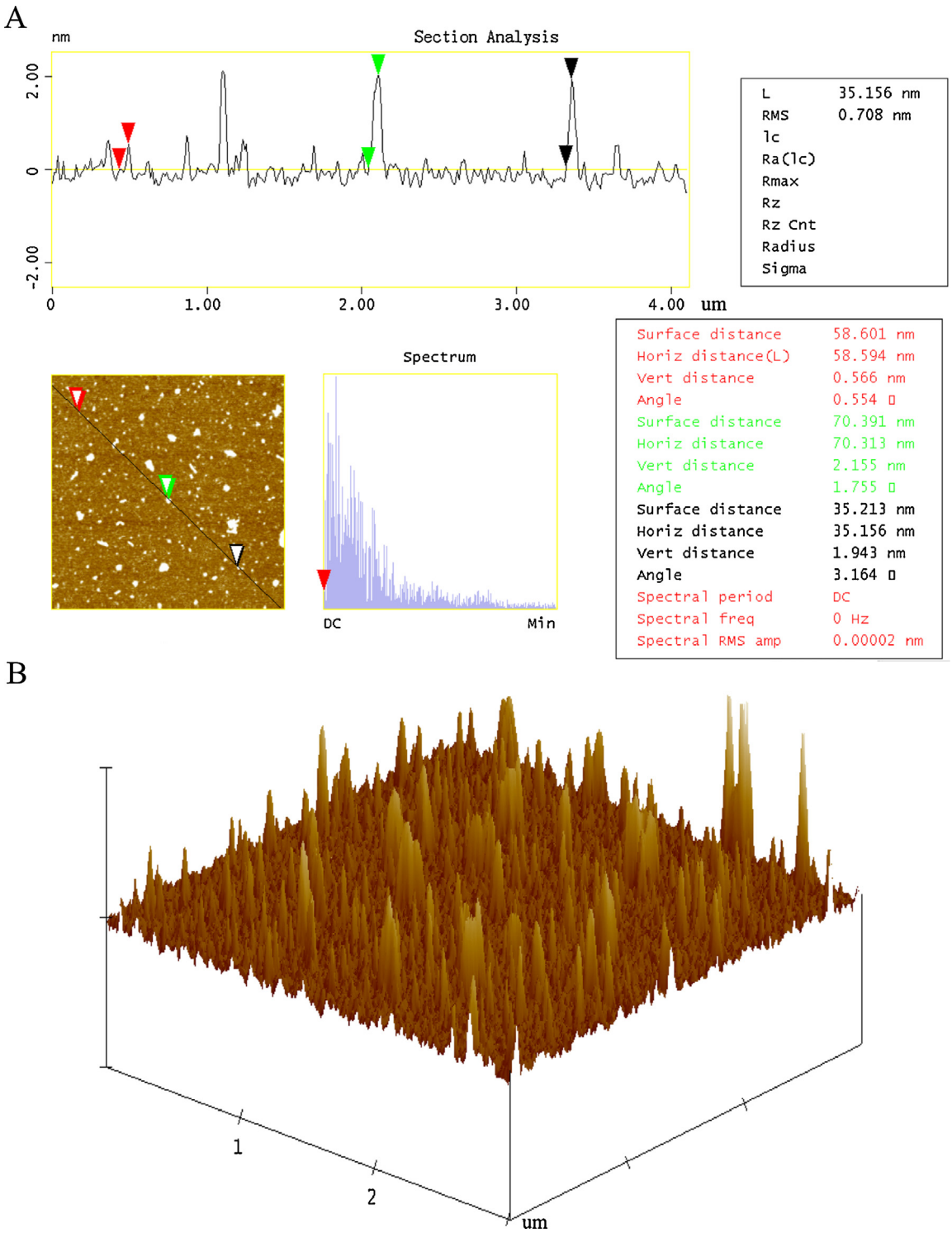

Fig. 6. AFM images of $SASP_{cata3}$ deposited from water at the concentration of 20 μg/mL. (A) 2D map and section analysis. Scale bar was 3 μm; inset height scale was 0–5 nm. (B) 3D map.

of hydroxyl radicals. This was in accordance with the result of Qi et al. that in the molecule of high DS, part of —OH groups were substituted by $—OSO_3H$ groups, so the scavenging effect was enhanced (Qi et al., 2005).

3.6.4. Reducing power

The reducing activities were usually related to the development of reductones, which terminate free radical chain reactions by donating a hydrogen atom (Qi et al., 2005). Reductones were also reported to react with certain precursors of peroxide, thus preventing peroxide formation. Fig. 7D depicted the reducing power of the samples and BHA. The reducing power values of $SASP_{cata2}$, $SASP_5$ and $SASP_1$ were 0.102, 0.036, 0.027 at 1 mg/mL, which were weaker than BHA. The reducing power of $SASP_{cata2}$ was relating more pronounced than that of the native one. Wang et al. reported that the reducing power of sulfated polysaccharides from *Laminaria japonica* was between 0.079 and 0.106 at the concentration of 1 mg/mL (Wang et al., 2008). Compared to the results, SASP had

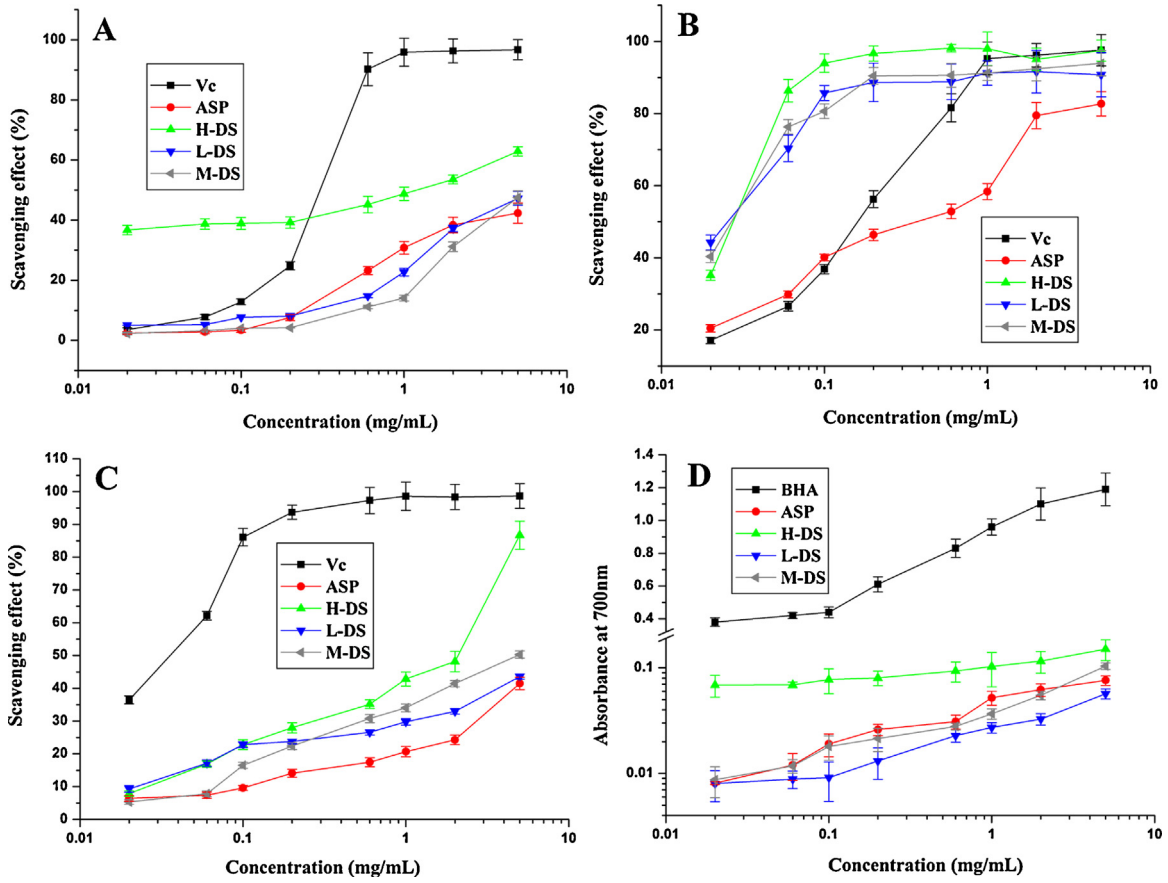

Fig. 7. Antioxidant effect of ASP and its sulfated derivatives. Samples with different DS were selected to evaluate antioxidant activities: H-DS ($SASP_{cata2}$, DS 1.24), M-DS ($SASP_5$, DS 0.91) and L-DS ($SASP_1$, DS 0.51). (A) Scavenging activity of DPPH radicals; (B) scavenging activity of superoxide radicals; (C) scavenging activity of hydroxyl radicals; (D) reducing power; data are presented as mean values ($n = 3$).

reducing capacity and the relation of reducing power to DS was significant.

Antioxidant activities of sulfated polysaccharides had been reported previously, but few investigations had been studied the effect of DS as an independent variable. It was interesting to note that the M_W of both $SASP_{cata2}$ and $SASP_1$ was similar but with different DS (Table 1). $SASP_{cata2}$ could achieve a significantly higher antioxidant activities than $SASP_1$ with lower DS. The possible reasons might be due to the supply of hydrogen by sulfated derivatives, which combined with radicals and formed a stable radical to terminate the radical chain reaction. This would be a new developmental direction for the synthesis of polysaccharide derivatives.

4. Conclusion

In the present study, sulfated derivatives of ASP with high DS were synthesized using DMAP/DCC as catalyst. According to the results of SEC-LLS, molecular parameters of ASP and SASP were calculated successfully from the experimental data of M_W and $\langle S^2 \rangle_z^{1/2}$. $SASP_{cata2}$ (DS of 1.24) exhibited an internal structure between rigid rod and random coil. The results revealed that the introduction of SO_3H groups improved significantly the stiffness of the chains due to the electrostatic effect. CD, MBS and CRS results also supported the idea of the rigid conformation in neutral or alkaline solutions. Furthermore, antioxidant experiments revealed that high DS could enhance the scavenging activities of radicals and reducing power of SASP in vitro. In summary, this work would give an insight that ASP after derivatization possessed better bioactivity, which will extend the biological applications of this natural polysaccharide. More work should be done to clarify the relationship between antioxidant activities and chemical structure such as substituent positions and different substituent groups.

Acknowledgments

Financial support of this research from National Science Foundation of China (21204073 and 51273162) is gratefully acknowledged. Financial supports of this research from Natural Science Foundation of Gansu Province (1308RJZA200) and Promotion Plan of Scientific Research Ability for Young Teachers from Northwest Normal University are also gratefully acknowledged. We would also like to thank Prof. Ruibin Guo (College of Chemistry & Chemical Engineering, Northwest Normal University) for the use of SEC-LLS.

References

Antonov, Y. A., & Sato, T. (2009). Macromolecular complexes of the main storage protein of *Vicia faba* seeds with sulfated polysaccharide. *Food Hydrocolloids*, *23*, 996–1006.

Bauer, J., & Burchard, W. (1993). Determination of scaling properties of randomly branched polycyanurates by combined SEC/LALLS/VISC. *Macromolecules*, *26*, 3103–3107.

Chen, X. Y., Xu, X. J., Zhang, L. N., & Kennedy, J. F. (2009). Flexible chain conformation of (1→3)-β-D-glucan from *Poria cocos* sclerotium in NaOH/urea aqueous solution. *Carbohydrate Polymers*, *75*, 586–591.

Chen, X. Y., Xu, X. J., Zhang, L. N., & Zeng, F. B. (2009). Chain conformation and anti-tumor activities of phosphorylated (1→3)-β-D-glucan from *Poria cocos*. *Carbohydrate Polymers*, *78*, 581–587.

Cui, H. X., Liu, Q., Tao, Y. Z., Zhang, H. F., Zhang, L., & Ding, K. (2008). Structure and chain conformation of a (1-6)-α-D-glucan from the root of *Pueraria lobata* (Willd.) Ohwi and the antioxidant activity of its sulfated derivative. *Carbohydrate Polymers*, *74*, 771–778.

Ghiselli, A., Nardini, M., Baldi, A., & Scaccini, C. (1998). Antioxidant activity of different phenolic fractions separated from an Italian red wine. *Journal of Agricultural Food and Chemistry*, *46*, 361–367.

Huang, X. L., Tan, Y. B., Zhou, Q. F., Wang, Y. X., & Che, Y. J. (2008). Aggregation behavior of sodium alginate with cucurbituril in aqueous solution. *Carbohydrate Polymers*, *74*, 685–690.

Liu, Y. H., Liu, C. H., Tan, H. N., Zhao, T., Cao, J. C., & Wang, F. S. (2009). Sulfation of a polysaccharide obtained from *Phellinus ribis* and potential biological activities of the sulfated derivatives. *Carbohydrate Polymers*, *77*, 370–375.

Marshall, L. F., Hoa, K. C., Peter, H. C., Madhav, P. Y., & Arland, T. H. (2009). Physicochemical characterization of alkaline soluble polysaccharides from sugar beet pulp. *Food Hydrocolloids*, *23*, 1554–1562.

Michon, C., Konate, K., Cuvelier, G., & Launay, B. (2002). Gelatin carrageenan interactions in coil and ordered conformations followed by a methylene blue spectrophotometric method. *Food Hydrocolloids*, *23*, 613–618.

Parvathy, K. S., Susheelamma, N. S., Tharanathan, R. N., & Gaonkar, A. K. (2005). A simple non-aqueous method for carboxymethylation of galactomannans. *Carbohydrate Polymers*, *62*, 137–141.

Qi, H. M., Zhang, Q. B., Zhao, T. T., Chen, R., Zhang, H., Niu, X. Z., et al. (2005). Antioxidant activity of different sulfate content derivatives of polysaccharide extracted from *Ulva pertusa* (Chlorophyta) in vitro. *International Journal of Biological Macromolecules*, *37*, 195–199.

Rout, D., Mondal, S., Chakraborty, I., & Islam, S. S. (2008). The structure and conformation of a water-insoluble (1→3)-,(1→6)-β-D-glucan from the fruiting bodies of *Pleurotus florida*. *Carbohydrate Research*, *343*, 982–987.

Shimada, K., Fujikawa, K., Yahara, K., & Nakamura, T. (1992). Antioxidative properties of xanthone on the auto oxidation of soybean in cylcodextrin emulsion. *Journal of Agricultural and Food Chemistry*, *40*(6), 945–948.

Sumihito, T., Tomoko, N., & Takashi, N. (2001). Ordered conformation of succinoglycan in aqueous sodium chloride. *Biomacromolecules*, *2*, 952–957.

Tao, F., Biao, G. Z., Yu, J. Z., & Ning, Z. H. (2008). Isolation and characterization of an acidic polysaccharide from Mesona Blumes gum. *Carbohydrate Polymers*, *71*, 159–169.

Tao, Y. Z., & Xu, W. L. (2008). Microwave-assisted solubilization and solution properties of hyperbranched polysaccharide. *Carbohydrate Research*, *343*, 3071–3078.

Tao, Y. Z., Zhang, L., & Peter, C. K. (2006). Physicochemical properties and antitumor activities of water-soluble native and sulfated hyperbranched mushroom polysaccharides. *Carbohydrate Research*, *341*, 2261–2269.

Tao, Y. Z., Zhang, L. N., Yan, F., & Wu, X. J. (2007). Chain conformation of water-insoluble hyperbranched polysaccharide from fungus. *Biomacromolecules*, *8*, 2321–2328.

Tomoko, N., & Takashi, N. (2003). Thermally induced conformation change of succinoglycan in aqueous sodium chloride. *Biomacromolecules*, *4*, 736–742.

Wang, J. G., Ma, Z. C., Zhang, L. N., Fang, Y. P., Jiang, F. T., & Phillips, J. O. (2011). Structure and chain conformation of water-soluble heteropolysaccharides from *Ganoderma lucidum*. *Carbohydrate Polymers*, *86*, 844–851.

Wang, J. L., Guo, H. Y., Zhang, J., Wang, X. F., Zhao, B. T., Yao, J., et al. (2010). Sulfated modification, characterization and structure–antioxidant relationships of *Artemisia sphaerocephala* polysaccharides. *Carbohydrate Polymers*, *81*, 897–905.

Wang, J. L., Niu, S. F., Zhao, B. T., Wang, X. F., Yao, J., Zhang, J., et al. (2013). Regioselective synthesis of sulfated guar gum: Comparative studies of structure and antioxidant activities. *International Journal of Biological Macromolecules*, *62*, 734–740.

Wang, J. L., Zhang, J., Wang, X. F., Zhao, B. T., Wu, Y. Q., & Yao, J. (2009). A comparison study on microwave-assisted extraction of *Artemisia sphaerocephala* polysaccharides with conventional method: Molecule structure and antioxidant activities evaluation. *International Journal of Biological Macromolecules*, *45*, 483–492.

Wang, X. H., Zhang, Y. Y., Zhang, L. N., & Ding, Y. W. (2009). Multiple conformation transitions of triple helical lentinan in DMSO/water by microcalorimetry. *Journal of Physical Chemistry B*, *113*, 9915–9923.

Wang, J., Zhang, Q. B., Zhang, Z. H., & Li, Z. (2008). Antioxidant activity of sulfated polysaccharide fractions extracted from *Laminaria japonica*. *International Journal of Biological Macromolecules*, *42*, 127–132.

Wang, J., Zhang, Q. B., Zhang, Z. S., Zhang, J. J., & Li, P. C. (2009). Synthesized phosphorylated and aminated derivatives of fucoidan and their potential antioxidant activity in vitro. *International Journal of Biological Macromolecules*, *44*, 170–174.

Wu, Y., Li, W., Cui, W., Eskin, N. A. M., & Goff, H. D. (2012). A molecular modeling approach to understand conformation-functionality relationships of galactomannans with different mannose/galactose ratios. *Food Hydrocolloids*, *26*, 359–364.

Xu, X. J., Chen, P., Wang, Y., & Zhang, L. N. (2009). Chain conformation and rheological behavior of an extracellular heteropolysaccharide Erwinia gum in aqueous solution. *Carbohydrate Research*, *344*, 113–119.

Xu, W. T., Zhang, F. F., Luo, Y. B., Ma, L. Y., Kou, X. H., & Huang, K. L. (2009). Antioxidant activity of a water-soluble polysaccharide purified from *Pteridium aquilinum*. *Carbohydrate Research*, *344*, 217–222.

Yang, L. Q., & Zhang, L. M. (2009). Chemical structural and chain conformational characterization of some bioactive polysaccharides isolated from natural sources. *Carbohydrate Polymers*, *76*, 349–361.

Yi, Y., Zhang, M. W., Liao, S. T., Zhang, R. F., Deng, Y. Y., Wei, Z. C., et al. (2012). Effects of alkali dissociation on the molecular conformation and immunomodulatory activity of longan pulp polysaccharide (LPI). *Carbohydrate Polymers*, *87*, 1311–1317.

Zhang, Y. Y., Li, S., Wang, X. H., Zhang, L. N., & Peter, C. K. C. (2011). Advances in lentinan: Isolation, structure, chain conformation and bioactivities. *Food Hydrocolloids*, *251*, 96–206.

Zhang, J., Wu, J., Liang, J. Y., Hu, Z. A., Wang, Y. P., & Zhang, S. T. (2007). Chemical characterization of Artemisia seed polysaccharide. *Carbohydrate Polymers*, *67*, 213–218.

Zhang, M., Zhang, L. N., Wang, Y. F., & Cheung, P. C. K. (2003). Chain conformation of sulfated derivatives of β-glucan from sclerotia of *Pleurotus tuber-regium*. *Carbohydrate Research*, *338*, 2863–2870.

Zou, C., Du, Y. M., Li, Y., Yang, J. H., Feng, T., Zhang, L., et al. (2008). Preparation of lacquer polysaccharide sulfates and their antioxidant activity in vitro. *Carbohydrate Polymers*, *73*, 322–331.